Nat Hazards (2016) 82:25–38
DOI 10.1007/s11069-016-2177-4

ORIGINAL PAPER

A wind tunnel study of sand-cemented bodies on wind erosion intensity and sand transport

Jie Zhou[1,2,3,4] · Jiaqiang Lei[1] · Shengyu Li[1] · Haifeng Wang[1] · Na Sun[1,3] · Xuexi Ma[1,3]

Received: 12 June 2015 / Accepted: 19 January 2016 / Published online: 29 January 2016

Abstract Wind tunnel experiments were used to test the capacity of sand-cemented bodies (SCB) on mulch beds. The total sand transport rate decreased as the level of SCB coverage increased. At higher SCB coverage (more than 40 %), the sand transport was basically unaffected by further increases in SCB coverage. While at low SCB coverage (less than 10 %), wind velocity played an important role in sand transport. Under the same SCB coverage, the sand transport depends on the increasing SCB size, due to the decrease in SCB density. The wind erosion intensity exponentially decreased with increasing SCB coverage (less than 40 %). The vertical profiles of horizontal mass flux from the SCB mulch–sand surface were also described by an exponential relationship. The vertical sand movement of particles was more sensitive to changes in SCB coverage at 20–40 %, compared with at less than 10 %. When the SCB coverage was more than 40 %, the decay rate of sand transport with height was nearly invariable. In summary, increases in SCB coverage had anti-erosion benefits for the underlying sand surface and could be considered for the development of a new type of sand fixation technology.

Keywords Sand-cemented bodies · Coverage · Wind erosion intensity · Sand transport

✉ Jiaqiang Lei
desert@ms.xjb.ac.cn

Jie Zhou
desert_zhoujie@163.com

[1] State Key Laboratory of Desert and Oasis Ecology, Xinjiang Institute of Ecology and Geography, Chinese Academy of Sciences, Ürümqi 830011, Xinjiang, China

[2] College of Resource and Environment Sciences, Xinjiang University, Ürümqi, Xinjiang, China

[3] University of Chinese Academy of Sciences, Beijing, China

[4] Cele National Station of Observation and Research for Desert-Grassland Ecosystem, Xinjiang Institute of Ecology and Geography, Chinese Academy of Sciences, Cele 848300, Xinjiang, China

1 Introduction

In arid and semi-arid regions, wind erosion is a major cause of environmental hazards. High-speed winds erode exposed surfaces, releasing dust that becomes suspended in the atmosphere, impacting on air quality (Husar et al. 2001) and human health (Schwartz 1994). Wind erosion, resulting in the detachment, transportation and re-deposition of soil particles, degrades soil productivity by removing the fertile topsoil and leads to serious deterioration of farmland (Overpeck et al. 1996; Husar et al. 2001; Schwartz 1994).

The most important two factors that influence the wind erosion process are the erosivity of the wind, erodibility of the soil, and the combined impact of erosivity and erodibility (Chepil and Woodruff 1963). Many studies have focused on how surface protrusions, such as vegetation and crop residues, can control soil loss from wind (Chepil 1944; Siddoway et al. 1965; Bisal and Ferguson 1970; Skidmore et al. 1979; Wasson and Nanninga 1986; Hagen 1996; Zhang et al. 2003; Guo et al. 2006; Li et al. 2007; Okin 2008; Blanco-Canqui 2010; Suter-Burri et al. 2013; Dupont et al. 2014). These studies reported that vegetation and crop residues could increase the threshold wind velocity that causes soil loss, by partially absorbing wind momentum and lowering the air forces on the erodible particles. In addition, the mass loss above the apparent threshold wind velocity can be remarkably decreased.

Gravel placed on top of sand is effectively non-erodible and increases the surface roughness, while enhancing the surface resistance; thus, gravel can play a similar role as vegetation or crop residues, in protecting topsoil from wind erosion. Gillette and Stockton (1989) revealed that non-erodible rough grains on erodible surfaces, such as coarse sand or gravel on arid surfaces, could reduce the degree of wind erosion. Liu et al. (1999) used wind tunnel experiments to demonstrate an exponential decrease in wind erosion with an increase in gravel coverage, when dispersed on an erodible bed. In addition, because of the low cost, compared with chemical sand-stabilizing materials or planting vegetation (Zhang et al. 2004), gravel mulches have been widely used in many other capacities, including shifting sand fixation, roadside erosion control and slope stabilization (Liu et al. 1999). Many studies have shown that other non-erodible materials (e.g. flat crop residues, standing residues, cotton gin trash and artificial clods) are also effective in reducing wind erosion potential (Chepil 1944; Fryear 1985; Bilbro and Fryrear 1994; Siddoway et al. 1965; Fryear and Koshi 1974; Chepil 1955).

The arid and semi-arid regions of the world are one of the primary sources of dust; the surface material of the Taklimakan Desert in China is loose, flowable and easy to corrode. Sand-cemented bodies (SCB) are naturally distributed on some inter-dune corridors in the central Taklimakan Desert. These bodies are continuously distributed across the region's inter-dune corridors, where they produce a layer of large granules combined with coarse sand covering the sand surface (Fig. 1). There has been little research into SCBs. However, SCBs are likely to decrease sand transport during wind flows. Their effectiveness needs to be determined, as SCBs have the potential to be used for sand control engineering.

SCB is cemented sand and looks like gravel. The average specific gravity of the SCB (2.486–2.534 g cm^{-3}) was close to gravel (2.65–2.75 g cm^{-3}). The SCBs were composed of a large number of sands with different particle sizes, and the main compositions of SCB were calcium sulphate (Sun et al. 2015). The shapes of the SCBs were very irregular and hard to distinguish (Fig. 2).

Considering that the SCBs are of a similar size and specific gravity to gravel, the question of whether they could be applied as a natural wind-resistant material on sandy

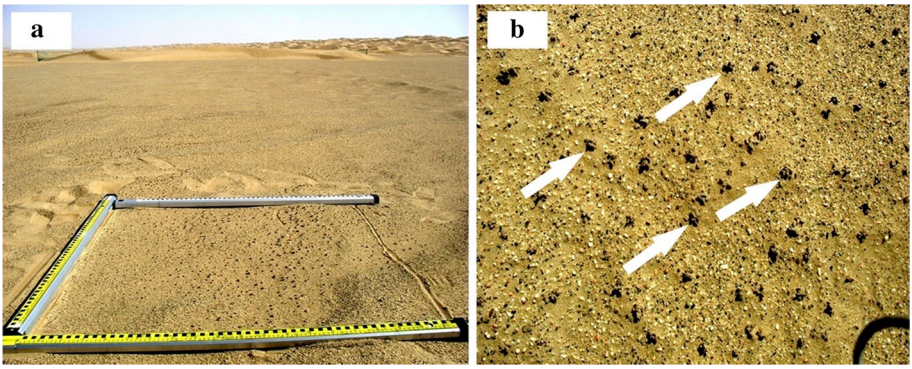

Fig. 1 Sand-cemented bodies lying on the sand surface in an inter-dune corridor within the central regions of the Taklimakan Desert: **a** a view of the SCB in relation to the surrounding landscape, and **b** a close-up of the SCB, which are marked by the *white arrows*

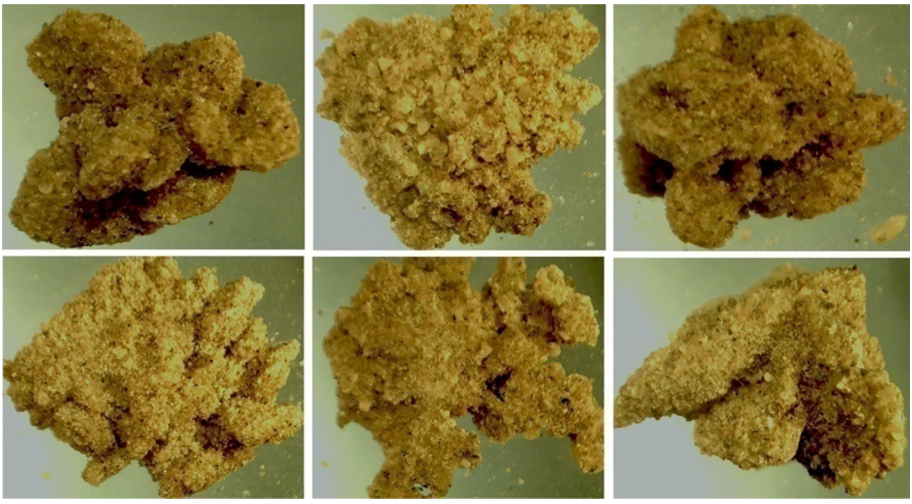

Fig. 2 The shapes of the SCB under the stereomicroscope (magnification: ×50)

surfaces was considered important. In this study, wind tunnel experiments were conducted using natural SCB and sand from the Taklimakan Desert. The objectives of this research were to (1) confirm the effect of SCBs in controlling sand movement and reducing the intensity of wind-induced soil erosion; (2) examine the height distribution function of aeolian sand transport in the presence of SCBs; and (3) present the rules governing the variation of sand transport rates with different levels of surface SCB coverage. The experiment provides a theoretical foundation for future sand control engineering and could be used to deepen our understanding of the mechanisms behind aeolian sand movement in desert terrains.

2 Materials and methods

2.1 Experimental design

Wind tunnel experiments were conducted in a blow-type non-circulating suction wind tunnel at the Xinjiang Institute of Ecology and Geography, Chinese Academy of Sciences. The wind tunnel had a total length of 16 m, and the 8-m-long working section had a cross-sectional area of 1 × 1.3 m. The wind velocity, of 1–25 m s^{-1}, could be adjusted continuously, and the boundary layer could be set 15–25 cm thick.

The experiment sand and SCB samples are collected from the central Taklimakan Desert. The sand samples were found to be composed primarily of silver sand and very fine sand, with the particle size of 0.1–0.05 mm (Wang et al. 2001). For keeping the similarity to field distribution of SCB mulch surface, the SCB samplers were directly used in wind tunnel experiment and without filtration after being gathered. The average and maximum dimensions of the SCBs were 8.6 and 13.5 mm, respectively. Seven different levels of percentage cover with the SCBs were considered: 0 % (control; CK), 2, 5, 8, 10, 20, 40 and 80 %. In order to determine the impact of SCB sizes on the sand transport rate, five different ranges of SCB dimensions were considered: 2–3, 3–5, 5–7, 7–10 and >10 mm. Each treatment combination was replicated three times at three wind speeds of 8, 10 and 15 m s^{-1}. The low wind speed of 8 m s^{-1} was chosen as the lower limit for this wind erosion investigation because very few sand particles moved at the threshold velocity 6 m s^{-1} and the amount of particles that did move did not satisfy the requirements for the present experiments. The middle wind speed of 10 m s^{-1} was chosen because it was representative of common wind events in the centre of the Taklimakan Desert (winds frequently reach 10 m s^{-1} for sustained periods within each season). The 15 m s^{-1} wind speed was chosen to represent a high wind event. Each treatment was subjected to the wind speed of 8 m s^{-1} for 10 min, 10 m s^{-1} for 5 min and 15 m s^{-1} for 3 min. Much of the erodible material was removed from the test surface within this time period.

To determine the variation of blown sand flux with height, the saltating sand transport at different heights along the downwind edge of the sand tray was measured using a vertical sand trap. The 20-cm-tall sand trap was sectioned into 1 × 1 cm openings to collect the blown sand at 20 heights (at 1-cm intervals). The sand trap was tested in the wind tunnel prior to use in this experiment and captured moving sand with a trap rate exceeding 90 %.

2.2 Calculations

The wind erosion intensity (Q; g m^{-2} min^{-1}) was defined as the mass (g) of the sand transported by the wind from a specified area (m^2) over a specified period of time (min). It was calculated as:

$$Q = \frac{(W_a - W_b)}{S * t} \tag{1}$$

where W_a and W_b represent the total weights (g) of the sand box before and after wind action, respectively, S is the area (m^2) of the sand plate, and t is the length of time (min) of wind action.

The sand flux profile of a blowing sand cloud was defined as the mass of sand transported by the wind within a unit flow layer, per unit width (perpendicular to the prevailing wind direction), per unit time:

$$q_z = q_0 \exp(-kz) \tag{2}$$

where q_z is the sand mass transport in g cm^{-2} s^{-1} at height z (cm), q_0 is defined as creeps at the surface ($z = 0$) sand mass transport (g cm^{-2} s^{-1}), and k is the decay coefficient.

3 Results and discussion

3.1 Total transport rate

3.1.1 Effect of sand-cemented body coverage levels and wind velocity on sand total transport rates

The total transport rates in terms of SCB coverage at the different wind velocities are plotted in Fig. 3. The total transport rates were not influenced much by the wind velocity on the sand surface, but they were strongly influenced by the level of SCB coverage. The gradients of the curves showing the relationship between the total transport rates and SCB coverages reflect the effect of the non-erodible particles on sand transport. The curves were characterized by three regions of differing gradients: when the SCB coverage was less than 20 %, the total transport rates decreased rapidly with increasing SCB coverage, while with SCB coverage between 20 and 40 %, there was a slight decrease in total transport rates with increasing SCB coverage, and above 40 % coverage, further increases in coverage had little effect on the total transport rates. At lower (<20 %) SCB coverage levels, the total transport rates also greatly increased when the wind velocity was higher. At the SCB coverage levels of 20–40 %, the effect of wind velocity was less pronounced, and when the SCB coverage was more than 40 %, the total transport rate was lower than 0.33 g cm^{-1} min^{-1} at all wind velocities. Al-Awadhi and Willetts (1999) and Li et al. (2013) similarly showed that when gravel coverage reached 50 % or more, total transport was basically unaffected by further increases in gravel coverage.

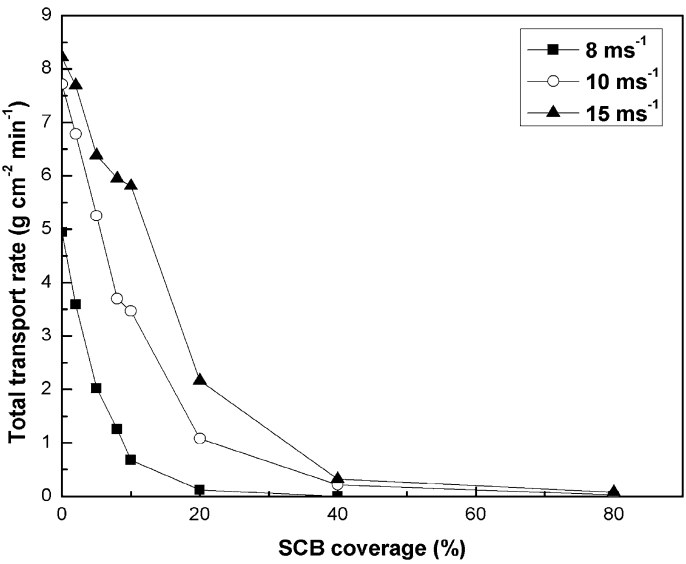

Fig. 3 The relationship between total transport rate and SCB coverage under different wind velocities

Figure 4 shows more clearly how the total transport rate increased with increasing wind velocity. The total transport rate is more sensitive to wind velocity at lower levels of SCB coverage. To further demonstrate this, the slopes of the curves in Fig. 4 reflect the relationship between the total transport rate and wind velocity under different levels of SCB coverage. At less than 10 % SCB coverage, the increase in the total transport rate with increasing wind velocity was large [mean slope (b) of curve: 0.55; Table 1]. Thus, under these conditions in the environment, changes in the wind velocity are likely to cause intense changes in the sand transport. This clearly shows that wind velocity plays an important role in sand transport when there are relatively low levels of SCB coverage.

When the SCB coverage reached 20 %, the slopes of the curves became smaller ($b = 0.28$; Table 1); thus, the surface SCB coverage intrinsically influenced the total transport rates. Increases in surface roughness and surface resistance, as well as the decrease in air flow momentum (due to the higher SCB coverage), are likely to have led to a higher erosion resistance of the surface sand. Hence, the increase in the total transport rate with wind velocity was low.

Finally, when the SCB coverage was more than 40 %, the total transport rate hardly increased with increasing wind velocity, shown by the very small slope of the curve (mean $b = 0.03$; Table 1). Clearly, the variation of the total transport rate at high levels of SCB coverage was steady and a stable surface that was not easily erodible had been created. Dong et al. (2002) found that the maximum aerodynamic roughness length occurred at gravel coverage levels ranging from 40 to 75 %, which implied that wind-eroded desert surfaces may even become stable when they are only partly covered by gravel. This explains why the total transport rate only decreased slightly when the SCB coverage was more than 40 %.

3.1.2 *Effect of sand-cemented body size on sand transport*

Figure 5 shows the effects of SCB size on the total transport rates, using the 20 % SCB coverage levels as an example. The total transport rates increased as the SCB size increased. This is in contrast to Li et al. (2013), who reported that an increase in gravel size

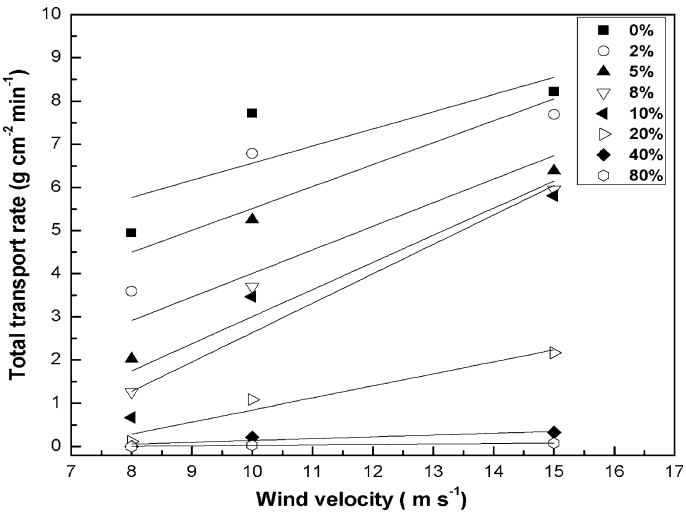

Fig. 4 The relationship between total transport rate and wind velocity at different levels of SCB coverage

Table 1 Linear fit ($y = a + b \times x$) of the relationship between total transport rate and wind velocity at different levels of SCB coverage

SCB coverage (%)	a (Intercept)	b (Slope)
0	2.59612	0.39678
2	0.43481	0.50794
5	−1.45988	0.54667
8	−3.28498	0.62897
10	−4.18447	0.68191
20	−1.93256	0.27775
40	−0.28086	0.04198
80	−0.08553	0.01092

(2, 3 and 5.5 cm) led to a reduction in sand transport from gravel beds, especially with low gravel coverage. This is because the large gravel could cause the interaction of gravel with saltation cloud to reduce the sand transport efficiency. In our study, the SCB size was much smaller than gravel size. Hence, it might make all the difference. In addition, the gaps were bigger in larger SCB particles than in smaller ones which could directly lead to the interaction of the wind with saltation sands increased. Logie (1981) and Nickling and Neuman (1995) found that low density of roughness elements led to increase in sand transport; they considered that the increase may have resulted from increasing surface shear stress (caused by the increases in roughness) and increases in the quantity of highly elastic collisions between the saltating sand particles and the roughness elements, which would have enhanced the particles' ejection and transport. The same low-density roughness elements may increase the localized shear stress and generate the turbulent eddies that continually result in scour around the elements (Gillies et al. 2006). According to a dimensional analysis of the fractions of wind stress absorbed by non-erodible roughness elements and intervening erodible soil (Minvielle et al. 2003), Raupach (1991) and

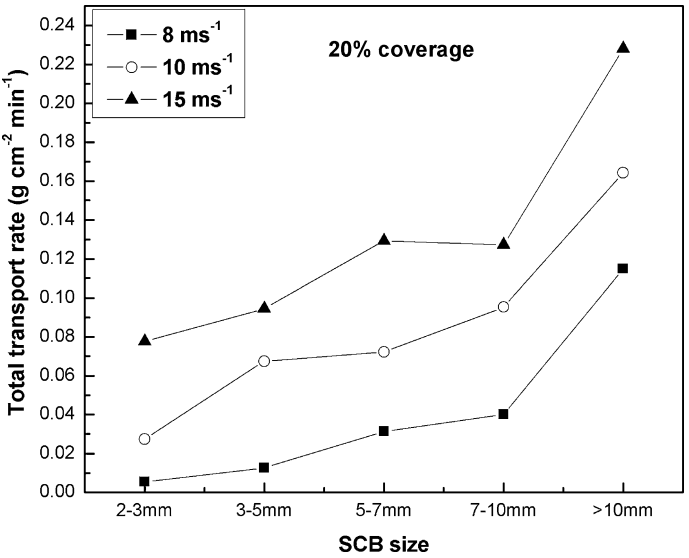

Fig. 5 Sand-cemented body size versus the total transport rates at 20 % SCB coverage levels

Table 2 The density (λ) of roughness elements at different SCB size distributions (n is the number of elements occupying the surface area, s, b is the element breadth, and h is the element height)

SCB size distribution (mm)	λ	n	b (cm)	h (cm)	S (cm^2)
2–3	0.48	4243	0.25	0.14	310.2
3–5	0.43	947	0.45	0.32	310.2
5–7	0.40	426	0.65	0.48	310.2
7–10	0.35	201	0.85	0.64	310.2
>10	0.18	59	1.15	0.85	310.2

Raupach et al. (1993) presented a parameterization of the threshold friction velocity as a function of the density of roughness elements (λ), defined as:

$$\lambda = nbh/s \tag{3}$$

where n is the number of elements occupying the surface area, s (cm^2), b is the element breadth (cm), and h is the element height (cm). Table 2 shows that at 20 % SCB coverage levels, λ decreases with the increase in particle size. Logie (1981) pointed that low densities of roughness elements tend to reduce the surface threshold velocity and cause increased erosion around the elements.

3.2 Wind erosion intensity at different levels of SCB coverage

Wind erosion occurred at all levels of SCB coverage, and the erosion intensity decreased gradually with increasing SCB coverage (Fig. 6). The CK treatment (0 % coverage) had the maximum wind erosion intensity, with the Q at 8, 10 and 15 m s^{-1} being 1966, 3842 and 4988 g m^{-2} min^{-1}, respectively. The 80 % coverage treatment had the minimum wind erosion intensity, with Q at 8, 10 and 15 m s^{-1} being 2, 8 and 39 g m^{-2} min^{-1}, respectively, that is, 0.1, 0.2 and 0.8 % of the CK. There was an exponential relationship between wind erosion intensity and the level of SCB coverage at each wind velocity, and the curve was characterized by three regions of different slopes. At an SCB coverage level of less than 20 %, the wind erosion intensity decreased rapidly with the increase in SCB coverage. For example, at 8 m s^{-1}, the wind erosion intensity was 1965.74 g m^{-2} min^{-1} in the CK treatment, but just 47.21 g m^{-2} min^{-1} in the 20 % SCB coverage treatment. Between SCB coverage levels of 20 and 40 %, the wind erosion intensity decreased more slowly, and at 8 m s^{-1}, the wind erosion intensity was 11.96 g m^{-2} min^{-1} in the 40 % SCB coverage. With further increases in the SCB coverage to 80 %, the wind erosion intensity decreased very slowly, so at 8 m s^{-1} wind velocity, the wind erosion intensity was 0.99 g m^{-2} min^{-1}. These results show that the variation in the wind erosion intensity tends to be steady, and the transportation of sand can be effectively controlled above 40 % SCB coverage. In previous studies, the recommended gravel coverage to form an equilibrated surface ranged from 40 to 80 % (Xue et al. 2000; Zhang et al. 2000, 2004; Wang et al. 2006). Our results indicate that an SCB mulch surface could have an effect similar to gravel mulch, in terms of controlling sand movement.

Wang et al. (2012) noted that wind speed had a larger effect on wind erosion intensity than gravel coverage, in terms of the aeolian sand movement. Figure 6 shows that at the same SCB coverage, the wind erosion intensity depends on wind speed. For example, at 20 % SCB coverage level, the wind erosion intensity was 47.21 and 890.29 g m^{-2} min^{-1}, respectively, at wind velocities of 8 and 15 m s^{-1} (the latter wind erosion intensity is 19

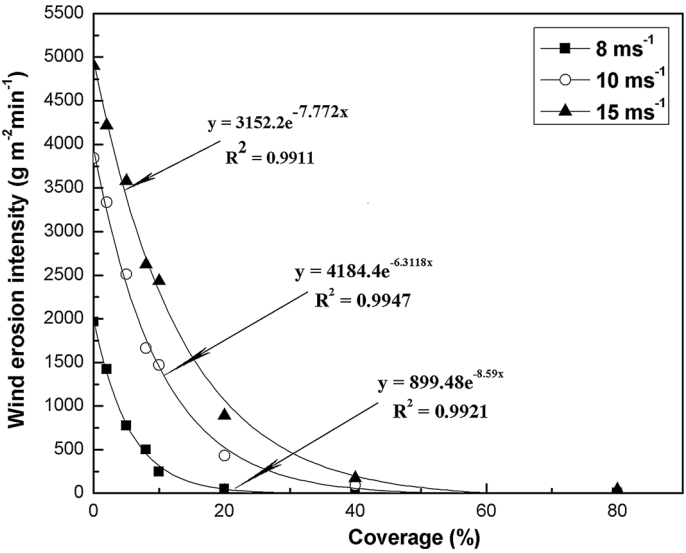

Fig. 6 Wind erosion intensity at different levels of SCB coverage and wind velocities

times greater than the former). While at an SCB coverage of 40 %, the wind erosion intensity was 12.07 and 170.87 g m^{-2} min^{-1}, respectively, at wind velocities of 8 and 15 m s^{-1} (here, the latter wind erosion intensity is 14 times greater than the former). These results also demonstrate that the greater the SCB coverage, the lower the wind erosion intensity. For example at wind velocity of 8 m s^{-1}, the wind erosion intensity was 47.21 and 12.07 g m^{-2} min^{-1}, respectively, at SCB coverage of 20 and 40 % (the former wind erosion intensity is about 4 times greater than the latter). While at 15 m s^{-1}, the wind erosion intensity was 890.29 and 170.87 g m^{-2} min^{-1}, respectively, at SCB coverage of 20 and 40 % (here, the former wind erosion intensity is 5 times greater than the latter).

3.3 Vertical profiles of horizontal mass flux at different SCB coverages and wind velocities

The vertical profiles of horizontal mass flux at different levels of SCB coverage and wind velocities are shown in Fig. 7. All mass flux profiles show a nearly exponential decay of q_z with height. At 0–2 cm height for the small coverage treatments (CK, 2, 5 and 8 %), the measured mass fluxes were less than those predicted by the exponential decay function. However, Butterfield (1999) used an optical sensor to make non-intrusive and highly accurate measurements of near-bed (<19 mm) sand transport profiles in a wind tunnel study; their results showed that sand transport near the bed dropped rapidly with height and that the curve did not inverse. Nickling and McKenna Neuman (1997) indicated that the airflows were most sensitive to distortion by intrusive sand traps in the near-bed region. Also, the SCB mulch surface in our study near the sand sampler may have some random properties such as airflow's pulsation and vortex. The creeping sands were easy to pile up at the front of the lowermost chamber of the sand traps due to its cohesion, which led the particles saltate to higher layer and this may greatly influence sand capture rate of near-bed region. Gillette and Stockton (1989) pointed out that the effect of non-erodible roughness

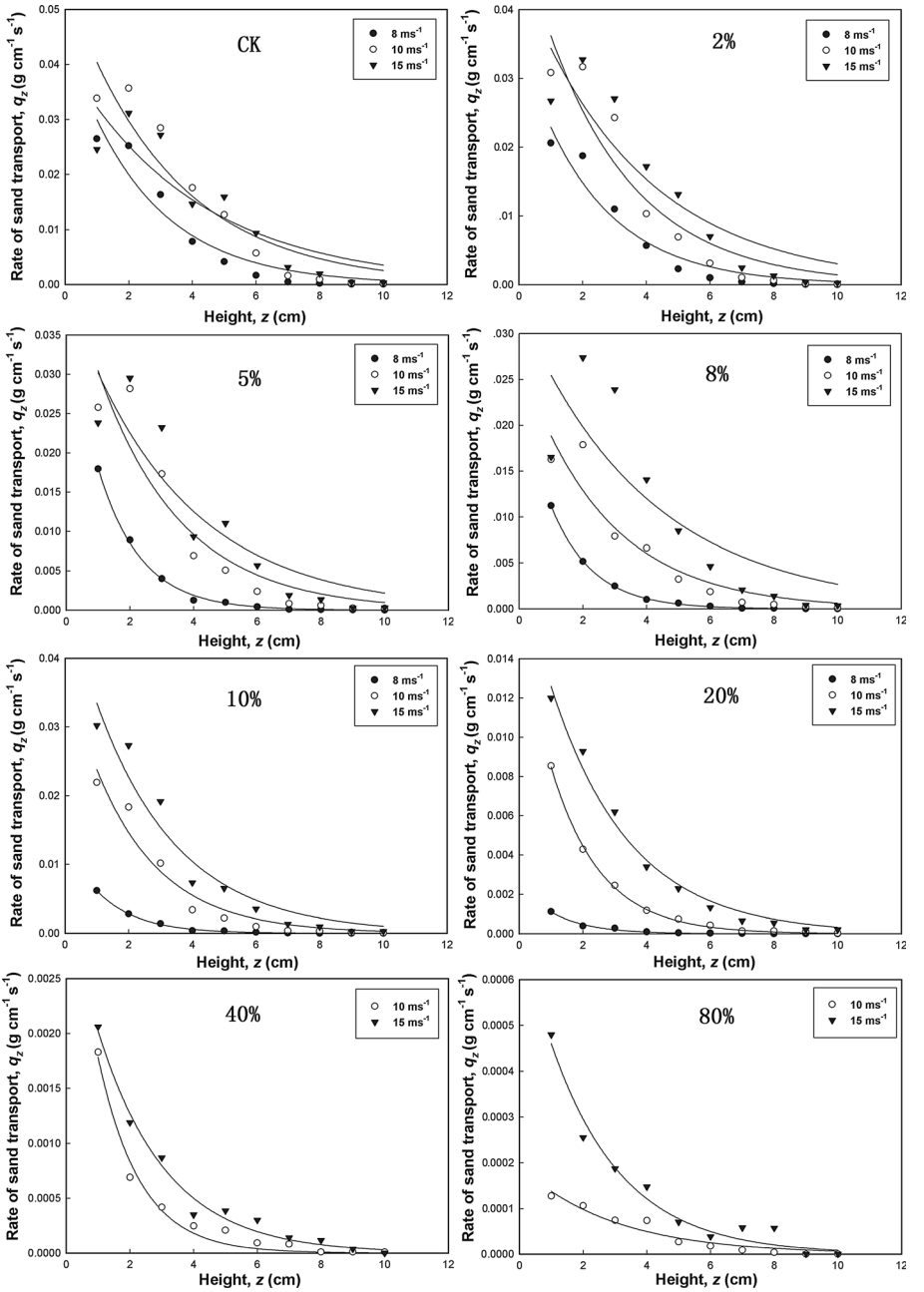

Fig. 7 Height variation of the horizontal mass flux of sediment at different SCB coverage levels and wind velocities

elements on a surface of erodible particles was to shelter part of that surface by absorption of part of the wind momentum flux. As the SCB coverage increased, the creeping sands would be decreased and the particles would move higher. Then, the SCB mulch bed's

resistance to surface aeolian erosion was enforced. As a result, the random properties of the SCB mulch bed near the sand sampler would have less influence. This explains why the inverse bending of the curve at 0–2 cm in this study did not occur with high SCB coverage.

The decay curves of sand transport on the SCB mulch sand bed can be expressed with an exponential equation (Eq. 2). From Table 3, we found that there was a strong correlation between sand mass transport and height, with high squared correlation coefficients (R^2) in most cases. Considering the sand transport profiles at different wind velocities and levels of SCB coverage, three sets curves were evident: (1) when the SCB coverage was less than 10 %, there was no appreciable change in the curve and the influence of coverage on the sand transport profile was minimal; (2) when the SCB coverage was between 10 and 40 %, the sand transport profile dropped quickly with height, especially at the bottom of the sand cloud, at a low wind velocity (8 m s^{-1}); and (3) when the SCB coverage was greater than 40 %, the sand transport profile decreased only slightly and sand transport did not occur at the lowest wind velocity (8 m s^{-1}). In addition, as the levels of SCB coverage increased, the sand transport profile was affected mainly at the bottom of the sand cloud.

Table 3 The flux profile of the sand cloud at different levels of SCB coverage and wind velocities

Coverage (%)	U (m s^{-1})	Q (g cm^{-1} s^{-1})	q_0	k	R^2
0	8	49.47	0.0449	0.4050	0.9335
	10	77.16	0.0549	0.3071	0.8995
	15	82.18	0.0412	0.2455	0.8162
2	8	35.92	0.0353	0.4345	0.9454
	10	67.82	0.0519	0.3592	0.9017
	15	76.91	0.0450	0.2693	0.8469
5	8	20.23	0.0384	0.7531	0.9980
	10	52.52	0.0447	0.3842	0.8975
	15	63.84	0.0405	0.2929	0.8414
8	8	12.52	0.0242	0.7694	0.9997
	10	36.96	0.0276	0.3797	0.9068
	15	59.51	0.0327	0.2502	0.7164
10	8	6.77	0.0136	0.7900	0.9982
	10	34.65	0.0387	0.4975	0.9549
	15	58.06	0.0493	0.3889	0.9457
20	8	1.19	0.0026	0.8399	0.9875
	10	10.82	0.0162	0.6443	0.9990
	15	21.65	0.0189	0.4051	0.9867
40	8	0	0	0	0
	10	2.15	0.0038	0.7600	0.9822
	15	3.26	0.0032	0.4654	0.9858
80	8	0	0	0	0
	10	0.26	0.0002	0.3392	0.9419
	15	0.77	0.0007	0.4447	0.9741

In the fitted function $q_z = q_0 \exp(-kz)$, q_z is the sand transport rate at height z; U is wind velocity; Q is the total transport rate at all height; q_0 and k are the regression coefficients; and R^2 is the correlation coefficient

As a result, the vertical movements of particles from surfaces with high SCB coverage (between 20 and 40 %) were more sensitive to changes in SCB coverage compared with those with low SCB coverage (less than 10 %). However, at the beds with higher SCB coverage (more than 40 %), the decay rate of sand transport with height was nearly invariable (Table 3).

4 Conclusion

A wind tunnel test using SCBs and sand from the central Taklimakan Desert was conducted, and the effects of surface SCB coverage on total transport rate, wind erosion intensity and the vertical profiles of horizontal mass flux were investigated. The total transport rates from the SCB mulch beds varied with SCB coverage and wind velocity. The gradients of the curves denoting the relationships between the total transport rates and SCB coverage at different wind velocities reflected the influences of the SCB mulch and wind velocities on the surface sand transport processes. When the SCB coverage was between 20 and 40 %, the total transport rates changed slowly with increasing SCB coverage, and the changes in the total transport rate were most sensitive to increasing wind velocities. When there was less than 10 % SCB coverage, the total transport rates increased with wind velocity very rapidly. These results showed that wind velocity plays an important role in sand transport. When the SCB coverage was more than 40 %, the total transport rates only dropped slightly with increasing coverage, which was demonstrated by the very small gradient of the curves, independent of wind velocity. Under these conditions, the sand transport was basically unaffected by the level of SCB coverage and the surface was not easily eroded.

At the same SCB coverage, the increases in the SCB size lead to an increase in sand transport from the SCB beds because the large particles were less dense (due to the low roughness element density) and the small particles were more dense (due to the high roughness element density) on the SCB beds.

There was an exponential relationship between the erosion intensity and level of SCB coverage; the greater the SCB coverage, the lower the wind erosion intensity. When the SCB coverage was more than 40 %, the transportation of sand transport was effectively controlled.

The vertical profiles of the horizontal mass flux on the SCB mulch sand surface were expressed with an exponential decay equation. The vertical movement of particles was more sensitive to changes in coverage variation at higher levels of SCB coverage (20–40 %), compared with lower levels of SCB coverage (less than 10 %). However, when the coverage was more than 40 %, the sand transport rate was basically impregnable.

Acknowledgments This study was supported by the fund of Mutual Feedback Mechanism of the Aeolian Landform Development with the Wind Field Characteristics (Grand No. 41201016).

References

Al-Awadhi JM, Willetts BB (1999) Sand transport and deposition within arrays of non-erodible cylindrical elements. Earth Surf Process Landf 24:423–435

Bilbro JD, Fryrear DW (1994) Wind erosion losses as related to plant silhouette and soil cover. Agron J 86(3):550–553

Bisal F, Ferguson WS (1970) Effect of non-erodible aggregates and wheat stubble on initiation of soil drifting. Can J Soil Sci 50(1):31–34
Blanco-Canqui H (2010) Energy crops and their implications on soil and environment. Agron J 102(2):403–419
Blumberg DG, Greeley R (1993) Field studies of aerodynamic roughness length. J Arid Environ 25:39–48
Butterfield GR (1999) Near-bed mass flux profiles in aeolian sand transport: high-resolution measurements in a wind tunnel. Earth Surf Process Landf 24:393–412
Chepil WS (1944) Utilization of crop residues for wind erosion control. Sci Agric 24(7):307–319
Chepil WS (1955) Factors that influence clod structure and erodibility of soil by wind. IV. Sand, silt and clay. Soil Sci 80:155–162
Chepil WS, Woodruff NP (1963) The physics of wind erosion and its control. Adv Agron 15:211–302
Dong Z, Liu X, Wang X (2002) Aerodynamic roughness of gravel surfaces. Geomorphology 43(1):17–31
Dupont S, Bergametti G, Simoëns S (2014) Modeling aeolian erosion in presence of vegetation. J Geophys Res Earth Surf 119(2):168–187
Fryear DW (1985) Soil cover and wind erosion. Trans ASAE (United States) 28(3):781–784
Fryear DW, Koshi PT (1974) Surface mulching with cotton gin trash improves sandy soils. USDA conservation research report 18
Gillette DA, Stockton PH (1989) The effect of nonerodible particles on wind erosion of erodible surfaces. J Geophys Res Atmos 94:12885–12893
Gillies JA, Nickling WG, King J (2006) Aeolian sediment transport through large patches of roughness in the atmospheric inertial sub layer. J Geophys Res Earth Surf (2003–2012) 111(F2):72-88
Guo YH, Zhao TN, Ding GD, Sun BP (2006) Influence of shrub coverage on the wind erosion of sandy soil. Res Soil Water Conserv 13:245–247
Hagen LJ (1996) Crop residue effects on aerodynamic processes and wind erosion. Theor Appl Climatol 54(1–2):39–46
Husar GM, Anziano DJ, Leuck M, Sebesta DP (2001) Covalent modification and surface immobilization of nucleic acids via the Diels–Alder bioconjugation method. Nucleosides Nucleotides Nucleic Acids 20(4–7):559–566
Li J, Okin GS, Alvarez L et al (2007) Quantitative effects of vegetation cover on wind erosion and soil nutrient loss in a desert grassland of southern New Mexico, USA. Biogeochemistry 85(3):317–332
Li H, Zhang W, Qu J et al (2013) Aeolian sand transport over Gobi with different gravel coverages under limited sand supply: a mobile wind tunnel investigation. Aeolian Res 11:67–74
Liu LY, Liu YZ, Li XY et al (1999) Effect of gravel mulch restraining soil deflation by wind tunnel simulation. J Desert Res 19(1):60–62
Logie M (1981) Wind tunnel experiments on dune sands. Earth Surf Process Landf 6:365–374
Minvielle F, Marticorena B, Gillette DA, Lawson RE, Thompson R, Bergametti G (2003) Relationship between the aerodynamic roughness length and the roughness density in cases of low roughness density*. Environ Fluid Mech 3(3):249–267
Nickling WG, Neuman CM (1995) Development of deflation lag surfaces. Sedimentology 42(3):403–414
Nickling WG, Neuman CM (1997) Wind tunnel evaluation of a wedge-shaped aeolian sediment trap. Geomorphology 18(3):333–345
Okin GS (2008) A new model of wind erosion in the presence of vegetation. J Geophys Res Earth Surf (2003–2012) 113(F2):1-11
Overpeck J, Anderson D, Trumbore S, Prell W (1996) The southwest Indian monsoon over the last 18000 years. Clim Dyn 12:213–225
Raupach MR (1991) Saltation layers, vegetation canopies and roughness lengths. Acta Mech 1(Suppl.):83–96
Raupach MR, Gillette DA, Leys JF (1993) The effect of roughness elements on wind erosion threshold. J Geophys Res Atmos 98(D2):3023–3029
Schwartz J (1994) Air pollution and daily mortality: a review and meta-analysis. Environ Res 64:36–52
Siddoway FH, Chepil WS, Armbrust DV (1965) Effect of kind, amount, and placement of residue on wind erosion control. Dissertation, Kansas State University
Skidmore EL, Kurnar M, Larson WE (1979) Crop residue management for wind erosion controll in the Great Plains. J Soil Water Conserv 34:90–96
Sun N, Li S, Ma X et al (2015) Wind tunnel experiment on the anti-erosion benefits of gravel-sized cemented bodies discovered on inter-dune corridor in central Taklimakan Desert. J Desert Res 36(4):2–6
Suter-Burri K, Gromke C, Leonard KC et al (2013) Spatial patterns of aeolian sediment deposition in vegetation canopies: observations from wind tunnel experiments using colored sand. Aeolian Res 8:65–73

Wang X, Dong Z, Chen G (2001) Characteristics of blown sand environment in middle Taklimakan Desert. J Desert Res 21(1):56–61

Wang W, Dong Z, Wang T, Zhang G (2006) The equilibrium gravel coverage of the deflated Gobi above the Mogao Grottoes of Dunhuang. China Environ Geol 50:1077–1083

Wang X, Lang L, Hua T et al (2012) Characteristics of the Gobi desert and their significance for dust emissions in the Ala Shan Plateau (Central Asia): an experimental study. J Arid Environ 81:35–46

Wasson RJ, Nanninga PM (1986) Estimating wind transport of sand on vegetated surfaces. Earth Surf Process Landf 11(5):505–514

Xue X, Zhang W, Wang T (2000) Wind tunnel experiments on the effects of gravel protection and problems of field surveys. Acta Geogr Sin 55:375–383 **(in Chinese, with English Abstract)**

Zhang W, Tao W, Xian X et al (2000) The discuss of comprehensively preventing blown-sand system in Mogao Grottoes, Dunhuang. J Desert Res 20:409–414

Zhang CL, Zou XY, Dong GR et al (2003) Wind tunnel studies on influences of vegetation on soil wind erosion. J Soil Water Conserv 17(3):31–33

Zhang W, Wang T, Wang W et al (2004) The Gobi sand stream and its control over the top surface of the Mogao Grottoes, China. Bull Eng Geol Environ 63:261–269